Carnegie Observatories Astrophysics Series, Vol. 4:
Origin and Evolution of the Elements, 2004
ed. A. McWilliam and M. Rauch (Cambridge: Cambridge Univ. Press)

Models of Chemical Evolution

FRANCESCA MATTEUCCI
University of Trieste, Astronomy Department, Trieste, Italy

Abstract

The basic principles underlying galactic chemical evolution and the most important results of chemical evolution models are discussed. In particular, the chemical evolution of the Milky Way galaxy, for which we possess the majority of observational constraints, is described. Then, it is shown how different star formation histories influence the chemical evolution of galaxies of different morphological type. Finally, the role of abundances and abundance ratios as cosmic clocks is emphasized and a comparison between model predictions and abundance patterns in high-redshift objects is used to infer the nature and the age of these systems.

1.1 Introduction

In order to build a chemical evolution model, one needs to specify some basic parameters such as the boundary conditions, namely whether the system is closed or open and whether the gas is primordial or already chemically enriched. Then one needs the stellar birthrate function, which is generally expressed as the product of two independent functions, the star formation rate (SFR) and the initial mass function (IMF),

$$B(m,t) = \psi(t)\varphi(m), \tag{1.1}$$

where the SFR is assumed to be only a function of time and the IMF only a function of the stellar mass. The stellar evolution and nucleosynthesis are also necessary ingredients for modeling chemical evolution, and in particular we need to specify the stellar yields $[p_i(m)]$.

Then, one can include in the chemical evolution model some supplementary ingredients such as the the infall of extragalactic material, radial flows, and galactic winds, which can play a more or less important role depending on the galactic system under study. In particular, gas infall and radial flows can be important in describing the chemical evolution of spiral disks, whereas galactic outflows are probably important in elliptical galaxies where the SFR was very high in the past and there is no cold gas at the present time, as well as in dwarf galaxies, which possess a smaller potential well. In fact, galactic outflows, which eventually can transform into galactic winds, are determined by two main processes: the supernova (SN) feedback, namely how much energy is transferred from SNe into the interstellar medium (ISM), and the galactic potential well.

In this paper, I will recall the most popular approximations used to describe both the basic and the supplementary ingredients involved in galactic chemical evolution. Then I will describe detailed numerical models that can follow the evolution in space and time of

the abundances of the most abundant chemical species. I will show some applications of such models to the Milky Way galaxy and then to galaxies of different morphological type, focusing on the fact that abundances and abundance ratios are very useful tools to infer the history of star formation in galaxies, to impose constraints on stellar nucleosynthesis, and to derive information on the nature and age of high-redshift objects.

1.2 The Star Formation Rate

The SFR is one of the most important drivers of galactic chemical evolution: it describes the rate at which the gas is turned into stars in galaxies. Since the physics of the star formation process is still not well known, several parameterizations are used to describe the SFR. A common aspect to the different formulations of the SFR is that they include a dependence upon the gas density. Here I recall the most commonly used parameterizations for the SFR adopted so far in the literature.

An exponentially decreasing SFR provides an easy-to-handle formula:

$$SFR = \nu e^{-t/\tau_*}, \tag{1.2}$$

with $\tau_* = 5-15$ Gyr in order to obtain a good fit to the properties of the solar neighborhood (Tosi 1988) and $\nu = 1-2\,\mathrm{Gyr}^{-1}$, being the so-called efficiency of star formation, which is expressed as the inverse of the time scale of star formation.

However, the most famous and most widely adopted formulation for the SFR is the Schmidt (1959) law:

$$SFR = \nu \sigma_{gas}^{k}, \tag{1.3}$$

which assumes that the SFR is proportional to some power of the volume or surface gas density. The exponent suggested by Schmidt was $k = 2$, but Kennicutt (1998) suggested that the best fit to the observational data on spiral disks and starburst galaxies is obtained with an exponent $k = 1.4 \pm 0.15$.

A more complex formulation, including a dependence also from the total surface mass density, which is induced by the SN feedback, was suggested by the observations of Dopita & Ryder (1994) who proposed the following formulation:

$$SFR = \nu \sigma_{tot}^{k_1} \sigma_{gas}^{k_2}, \tag{1.4}$$

with $1.5 < k_1 + k_2 < 2.5$.

Kennicutt suggested also an alternative law to the Schmidt-like one discussed above, in particular a law containing the angular rotation speed of gas, Ω_{gas}:

$$SFR = 0.017 \Omega_{gas} \sigma_{gas} \propto R^{-1} \sigma_{gas} \tag{1.5}$$

A similar law for the SFR taking into account star formation induced by spiral density waves was proposed by Wyse & Silk (1989), and it can be expressed as (Prantzos 2003):

$$SFR = \nu V(R) R^{-1} \sigma_{gas}^{1.5}, \tag{1.6}$$

where $V(R)$ is the rotational velocity in the disk and R is the galactocentric distance. It is worth noting that the SFRs expressed by Equations (1.4)–(1.6) contain a stronger dependence on the radial properties of the disk than the simple Schmidt law, and this characteristic is required to best fit the disk properties (see next sections).

1.3 The IMF

The most common parameterization for the IMF is that proposed by Salpeter (1955), which assumes a one-slope power law with $x = 1.35$, such that

$$\varphi(M) = cM^{-(1+x)} \tag{1.7}$$

is the number of stars with masses in the interval M to $M + dM$, and c is a normalization constant.

The IMF is generally normalized as

$$\int_0^\infty M\varphi(M)dM = 1. \tag{1.8}$$

More recently, multi-slope (x_1, x_2,...) expressions of the IMF have been adopted since they better describe the luminosity function of the main sequence stars in the solar vicinity (Scalo 1986, 1998; Kroupa, Tout, & Gilmore 1993). Generally, the IMF is assumed to be constant in space and time, with some exceptions such as the one suggested by Larson (1998), who adopts a variable slope:

$$x = 1.35(1 + m/m_1)^{-1}, \tag{1.9}$$

where m_1 is variable with time and associated with the Jeans mass. The effects of a variable IMF on the Galactic disk properties have been studied by Chiappini, Matteucci, & Padoan (2000), who concluded that only a very *ad hoc* variation of the IMF can reproduce the majority of observational constraints, thus favoring chemical evolution models with an IMF constant in space and time.

1.4 Infall and Outflow

Depending on the galactic system, the infall rate can be assumed to be constant in space and time, or, more realistically, the infall rate can be variable in space and time:

$$IR = A(R)e^{-t/\tau(R)}, \tag{1.10}$$

with $\tau(R)$ constant or varying along the disk. The parameter $A(R)$ is derived by fitting the present-day total surface mass density in the disk of the Galaxy, $\sigma_{tot}(t_G)$. Otherwise, for the formation of the Galaxy one can assume two independent episodes of infall during which the halo and perhaps part of the thick disk formed first, followed by the thin disk. As in the two-infall model of Chiappini, Matteucci, & Gratton (1997),

$$IR = A(R)e^{-t/\tau_H(R)} + B(R)e^{-(t-t_{max})/\tau_D(R)} \quad . \tag{1.11}$$

Here $\tau_H(R)$ is the time scale for the formation of the halo/thick disk and $\tau_D(R)$ is the time scale for the formation of the thin disk. The latter is assumed to increase linearly with galactocentric distance (Matteucci & François 1989; Chiappini et al. 1997; Boissier & Prantzos 1999). There are no specific prescriptions for the rate of gas outflow or galactic wind, but generally one simply assumes that the wind rate is proportional to the star formation rate through a suitable parameterization (Hartwick 1976; Matteucci & Chiosi 1983):

$$W = -\lambda SFR, \tag{1.12}$$

with λ being a free parameter.

1.5 Stellar Yields

The stellar yields are fundamental ingredients in galactic chemical evolution. In order to introduce the stellar yields, we recall some useful concepts and define the *yield per stellar generation*.

Under the assumption of "instantaneous recycling approximation," we define the yield per stellar generation of a given element i as (Tinsley 1980):

$$y_i = \frac{1}{1-R} \int_{m_1}^{\infty} m p_{im} \varphi(m) dm \tag{1.13}$$

where p_{im} is the stellar yield of the element i, namely the newly formed and ejected mass fraction of the element i by a star of initial mass m, and m_1 is the turn-off mass of the stellar generation. It is worth noting that the expression (1.13) is an oversimplification, and it does not have much meaning when considering chemical elements formed on long time scales. The quantity R is the returned fraction:

$$R = \int_{m_1}^{\infty} (m - M_{rem}) \varphi(m) dm, \tag{1.14}$$

where M_{rem} is the remnant mass of a star of mass m. In the past 10 years a large number of calculations of the stellar yields have become available for stars of all masses and metallicities. However, uncertainties in stellar yields are still present, especially in the yields of Fe-peak elements. This is due to uncertainties in the nuclear reaction rates, treatment of convection, mass cut, explosion energies, neutron fluxes and possible fall-back of matter on the proto-neutron star. Moreover, the ^{14}N nucleosynthesis and its primary and/or secondary nature are still under debate. The most recent calculations are summarized below.

- Low- and intermediate-mass stars ($0.8 \leq M/M_{\odot} \leq 8.0$) produce ^{4}He, C, N and some *s*-process ($A > 90$) elements (Marigo, Bressan, & Chiosi 1996; van den Hoeck & Groenewegen 1997; Meynet & Maeder 2002; Siess, Livio, & Lattanzio 2002; Ventura, D'Antona, & Mazzitelli 2002).
- Massive stars ($M \geq 10 M_{\odot}$) produce mainly α-elements (O, Ne, Mg, Si, S, Ca), some Fe-peak elements, *s*-process elements ($A < 90$), and *r*-process elements (Langer & Henkel 1995; Woosley & Weaver 1995; Thielemann, Nomoto, & Hashimoto 1996; Nomoto et al. 1997; Rauscher, Hoffman, & Woosley 2002; Limongi & Chieffi 2003).
- SNe Ia produce mainly Fe-peak elements (Nomoto et al. 1997; Iwamoto et al. 1999).
- Very massive objects ($M > 100 M_{\odot}$), if they exist, should produce mostly oxygen (Portinari, Chiosi, & Bressan 1998; Nakamura et al. 2001; Umeda & Nomoto 2002).

In Figures 1.1 and 1.2 we show a comparison between the yields, produced in massive stars, of two α-elements (O and Mg) and Fe, respectively, as predicted by different authors. As is evident from Figure 1.1, the O yields from different sources seem to be in good agreement with one another. The yields of Mg, especially the most recent ones, seem to be also in good agreement with each others, whereas for the yields of Fe (Fig. 1.2) there is not yet an agreement among different authors. Observational estimates of Fe produced in Type II supernovae (SNe II) (Elmhamdi, Chugai, & Danziger 2003) can help in constraining the Fe yields in massive stars.

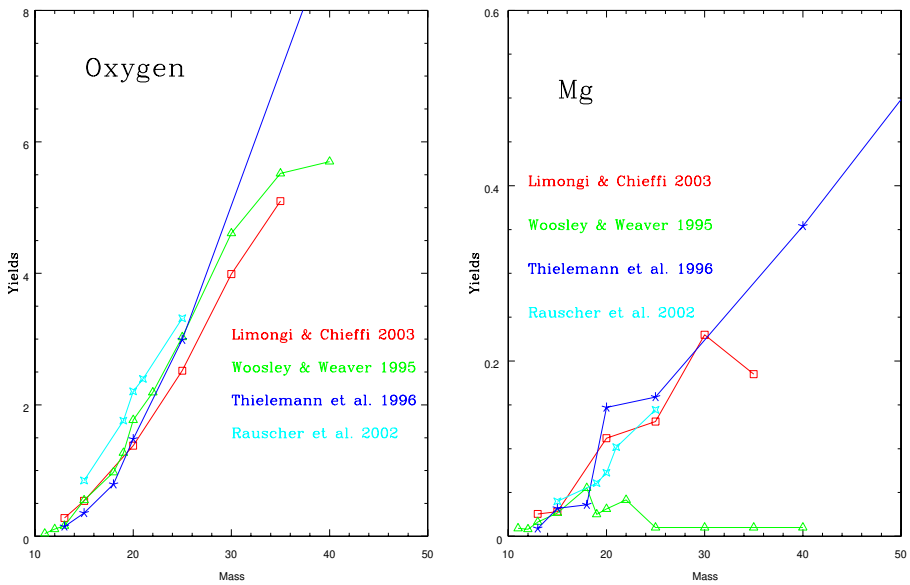

Fig. 1.1. Comparison between different yields of O and Mg from SNe II: open triangles, Woosley & Weaver (1995); open squares, Limongi & Chieffi (2003); stars, Thielemann et al. (1996); four-point stars, Rauscher et al. (2002).

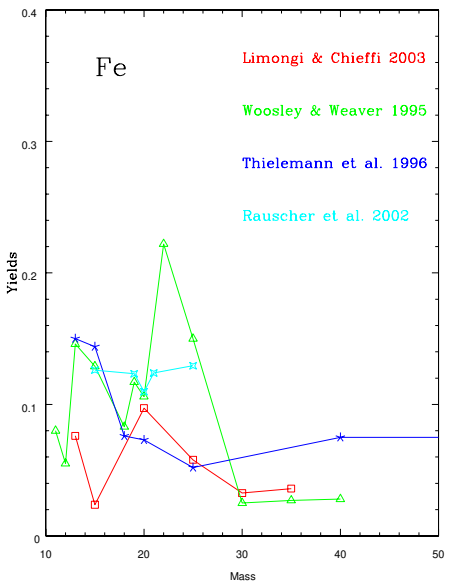

Fig. 1.2. Comparison between different yields of Fe from SN II: open triangles, Woosley & Weaver (1995); open squares, Limongi & Chieffi (2003); stars, Thielemann et al. (1996); four-point stars, Rauscher et al. (2002).

1.6 Analytical Models of Chemical Evolution

The simplest model of galactic chemical evolution is the so-called *Simple Model* for the evolution of the solar neighborhood. We define the solar neighborhood or solar vicinity as a cylinder centered on the Sun with 1 kpc radius.

The basic assumptions of the Simple Model can be summarized as follows:

- The system is one-zone and closed, no inflows or outflows
- The initial gas is primordial (no metals)
- The instantaneous recycling approximation holds
- $\varphi(m)$ is constant in time and space
- The gas is well mixed at any time (instantaneous mixing approximation)

Let X_i be the abundance of an element i and $\beta = \frac{M_{gas}}{M_{tot}}$ be the ratio between the mass of gas and the total mass of the system. If $X_i \ll 1$, which is generally true for metals, then we can write:

$$X_i = y_i \ln(\frac{1}{\beta}), \tag{1.15}$$

which is the well-known solution for the Simple Model, where y_i is the yield per stellar generation as defined in Equation (1.13). In particular, the yield appearing in Equation (1.15) is usually referred to as the *effective yield*. If X_i is not much lower than 1, as is the case for $X_{\rm He}$ (Maeder 1992), a more precise expression for the solution of the Simple Model is given by

$$X_i = 1 - \beta^{y_i} \quad . \tag{1.16}$$

It is worth noting that in the instantaneous recycling approximation we can generally assume

$$\frac{X_i}{X_j} = \frac{y_i}{y_j}, \tag{1.17}$$

namely that the abundance ratios are equivalent to the yield ratios, and this holds also in analytical models with infall and/or outflow. Clearly, Equation (1.17) can be used safely only for elements produced on short time scales, such as α-elements, but it fails if applied to elements produced on long time scales, such as Fe and N. These days the Simple Model is rarely used in describing the chemical evolution of the Milky Way since it does not reproduce the G-dwarf metallicity distribution (the G-dwarf problem) as well as the elements produced on long time scales such as Fe (Matteucci 2001).

1.7 Numerical Models of Chemical Evolution

In the last few years, a great number of models relaxing the instantaneous recycling approximation and the closed box assumptions, but retaining the constancy of the IMF and the instantaneous mixing approximation, have appeared in the literature. As an example of the basic equations adopted in such models, I show the formulation of Matteucci & Greggio (1986), which is based on the original formulations of Talbot & Arnett (1971) and Chiosi (1980).

Letting G_i be the mass fraction of gas in the form of an element i $[\sigma_i/\sigma_{tot}(t_G)]$, we can write

$$\dot{G}_i(t) = -\psi(t)X_i(t) + \int_{M_L}^{M_{Bm}} [\psi(t-\tau_m)Q_{m1i}X_i(t-\tau_{m2})d\mu]dm$$
$$+A\int_{M_{Bm}}^{M_{BM}} \phi(m)\cdot[\int_{\mu_{min}}^{0.5} f(\mu)\psi(t-\tau_{m2})Q_{mi}X_i(t-\tau_{m2})d\mu dm$$
$$+(1-A)\int_{M_{Bm}}^{M_{BM}} \psi(t-\tau_m)Q_{mi}X_i(t-\tau_m)\phi(m)dm$$
$$+\int_{M_{BM}}^{M_U} \psi(t-\tau_m)Q_{mi}X_i(t-\tau_m)\phi(m)dm + X_{A_i}IR(t) - X_iW(t), \quad (1.18)$$

where A is a constant parameter chosen in order to fit the present-day SN Ia rate and it lies in the range $0.05 < A < 0.09$. The SN Ia rate should be based on the existing theories on SN Ia progenitors, which I will summarize in the next section. In the equations above the Type Ia SNe (SNe Ia) are assumed to originate from C-O white dwarfs (WDs) in binary systems, and $f(\mu)$ represents the distribution of mass ratios in such binary systems ($\mu = \frac{m_2}{(m_1+m_2)}$). The quantities m_1 and m_2 are the primary and the secondary mass of the binary system, respectively. The primary star of the system is the exploding WD, which contributes to the nucleosynthesis products of the SN Ia explosion, whereas the secondary star is the clock of the system. In other words, the SN Ia occurs when the secondary evolves off the main sequence and transfers material on the companion. Therefore, τ_{m_2} is the lifetime of the secondary star and the clock of the explosion. The integral that calculates the material restored by SNe Ia is made over the range of total masses of the binary systems that are supposed to give rise these SNe. In particular, $M_{Bm} = 3M_\odot$ is the minimum mass for such a binary system and $M_{BM} = 16M_\odot$ is the maximum (see Matteucci & Greggio 1986 and Matteucci & Recchi 2001 for details). The masses M_L and M_U represent the minimum mass contributing to galactic chemical enrichment at a given time and the maximum assumed mass for stars, respectively. The quantities Q_{mi} and Q_{m1i} are production matrices that take into account all the nucleosynthesis products ejected by a star of mass m and m_1, respectively (see Matteucci 2001 for details).

The star formation rate $\psi(t)$ and all the rates in this equation are expressed as functions of the fraction of gas [$G = \frac{\sigma_{gas}}{\sigma_{tot}(t_G)}$]. The quantities $IR(t)$ and $W(t)$ represent the rate of gas accretion and the rate of galactic outflow (wind), respectively, and X_{A_i} are the abundances of the accreting material, which are usually assumed to be primordial (no metals). Generally, in describing the solar neighborhood and the Galactic disk one assumes $W(t) = 0$, whereas the infall of mostly primordial material is most likely to be responsible for the formation of the disk.

1.7.1 SN Ia Progenitors

The "single degenerate" scenario is the classical scenario originally proposed by Whelan & Iben (1973), namely C-deflagration in a C-O WD reaching the Chandrasekhar mass limit, $M_{\rm Ch} \approx 1.44M_\odot$, after accreting material from a red giant companion. The progenitors of C-O WDs lie in the range $0.8-8.0M_\odot$; therefore, the most massive binary system of two C-O WDs is the $8M_\odot + 8M_\odot$ one. The clock of the system in this scenario is provided by the lifetime of the secondary star (i.e. the less massive one in the binary system).This implies that the minimum time scale for the appearance of the first SNe Ia is the lifetime of the

most massive secondary star. In this case the time is $t_{SNIa_{min}}$ = 0.03 Gyr (Greggio & Renzini 1983a; Matteucci & Greggio 1986; Matteucci & Recchi 2001).

The "double degenerate" scenario consists in the merging of two C-O WDs due to loss of angular momentum occurring as a consequence of gravitational wave radiation, which then explode by C-deflagration when $M_{\rm Ch}$ is reached (Iben & Tutukov 1984). In this case the minimum time scale for the appearance of SNe Ia is the lifetime of the most massive secondary star plus the gravitational time delay, which depends on the original separation of the two WDs and which is computed according to Landau & Lifshitz (1962), namely $t_{SNIa_{min}} = 0.03 + \Delta t_{grav} = 0.03 + 0.15$ Gyr (Tornambè & Matteucci 1986). We recall that the gravitational time delay can be as long as several Hubble times.

The model by Hachisu, Kato, & Nomoto (1999) is based on the classical scenario of Whelan & Iben (1973), but with a metallicity effect implying that no SNe Ia systems can form for [Fe/H]< -1.0 in the ISM. This implies a much longer time delay for the first SNe Ia to occur, also because the maximum masses of the secondary stars in the binary systems are assumed to be $\leq 2.6 M_{\odot}$. Therefore, in this case $t_{SNIa_{min}} = 0.33$ Gyr + metallicity delay due to the chemical evolution of the considered system. In this scenario, SNe Ia are not associated with young stellar populations, contrary to what is suggested by a recent search for SNe Ia in starburst galaxies (see Mannucci et al. 2003), which seem to favor the scenario where the progenitors of SNe Ia can be as high as 8 $M_{\odot}$.

Clearly, $t_{SNIa_{min}}$ is a very important parameter for computing galactic chemical evolution since the abundance patterns will depend strongly on this time scale, although the most important time scale is the one for which the SNe Ia have an impact on the abundances of the ISM. In successful models of galactic chemical evolution of the solar vicinity this time scale is 1.0–1.5 Gyr in the framework of the single degenerate model (Matteucci & Greggio 1986). In the other two scenarios this time is longer, especially in the one including the metallicity effect and it varies with different histories of star formation (see Matteucci & Recchi 2001 and § 1.13).

1.8 Different Approaches to the Formation and Evolution of the Galaxy

In the past years, several approaches to the calculation of the chemical evolution of the Galaxy were proposed.

(1) *Serial formation:* The halo, thick disk, and thin disk form in a sequence as a continuous process (e.g., Matteucci & François 1989).

(2) *Parallel formation:* The various Galactic components start forming at the same time and from the same gas but evolve at different rates. This approach predicts overlapping of stars belonging to the different components (e.g., Pardi, Ferrini, & Matteucci 1995), but it does not provide a simultaneously good fit to the G-dwarf metallicity distribution and the halo star metallicity distribution, as discussed in Matteucci (2001).

(3) *The two-infall approach:* The halo and disk form out of two separate infall episodes from extragalactic gas. Also in this case we predict an overlap in metallicity between the different Galactic components (e.g., Chiappini et al. 1997; Chang et al. 1999). A threshold density ($\sigma_{th} = 7 M_{\odot}$ pc^{-2}) in the star formation process is also included in the model of Chiappini et al. (1997).

(4) *The stochastic approach:* The assumption is made that in the early halo phases mixing was not efficient and pollution from single SNe would dominate the Galactic enrichment (Tsujimoto, Shigeyama, & Yoshii 1999; Argast et al. 2000; Oey 2000). In this case a

large spread in the abundances and abundance ratios at low metallicities is predicted. This predicted spread, however, is much larger than observed, especially for α-elements.

1.9 Observational Constraints

A good model of chemical evolution should be able to reproduce a maximum number of observational constraints, and the number of observational constraints should be larger than the number of free parameters, which are τ_H, τ_D, k_1, k_2, ν, the IMF slope(s), and the parameter describing the wind, if adopted.

The main observational constraints in the solar vicinity that a good model should reproduce (see Boissier & Prantzos 1999; Chiappini, Matteucci, & Romano 2001) are:

- The present-day surface gas density: $\Sigma_G = 13 \pm 3 M_\odot$ pc^{-2}
- The present-day surface star density: $\Sigma_* = 43 \pm 5 M_\odot$ pc^{-2}
- The present-day total surface mass density: $\Sigma_{tot} = 51 \pm 6 M_\odot$ pc^{-2}
- The present-day SFR: $\psi_o = 2-5 M_\odot$ pc^{-2} Gyr^{-1}
- The present-day infall rate: $0.3-1.5 M_\odot$ pc^{-2} Gyr^{-1}
- The present-day mass function
- The solar abundances, namely the chemical abundances of the ISM at the time of birth of the solar system 4.5 Gyr ago and the present-day abundances
- The observed [X_i/Fe] vs. [Fe/H] relations
- The G-dwarf metallicity distribution
- The age-metallicity relation

And finally, a good model of chemical evolution of the Milky Way should reproduce the distributions of abundances, gas and star formation rate along the disk, as well as the average SN II and SN Ia rates along the disk [1.2 ± 0.8 (100 yr)$^{-1}$ for SNe II and 0.3 ± 0.2 (100 yr)$^{-1}$ for SNe Ia].

1.10 Time-delay Model Interpretation

The difference in the time scales for the occurrence of SNe II and SNe Ia produces a time delay in the Fe production relative to the α-elements (Tinsley 1979; Greggio & Renzini 1983b; Matteucci 1986). On this basis we can interpret all the observed abundance ratios plotted as functions of metallicity. In particular, this interpretation is known as the time-delay model and can be easily illustrated by Figure 1.3, where we show the predictions of the two-infall model for the chemical evolution of the solar vicinity concerning the [O/Fe] vs. [Fe/H] relation. We show the standard case in which the contributions to Fe enrichment from both SNe II and SNe Ia are taken into account, as well as the cases where only one type of SNe at a time is assumed to contribute to Fe enrichment. Both data and models are normalized to the meteoritic solar abundances (Anders & Grevesse 1989). From Figure 1.3, it is evident that only SNe Ia as Fe producers would predict a continuous decrease of the [O/Fe] ratio from low to high metallicities (upper curve), whereas only SNe II would create a roughly constant [O/Fe] ratio. Therefore, only a model including both contributions in the percentages of 30% (SNe II) and 70% (SNe Ia) can reproduce the data.

The time-delay model, with the assumption of an IMF constant in time, can explain the different abundance patterns in the halo, disk, and bulge (see Matteucci 2001).

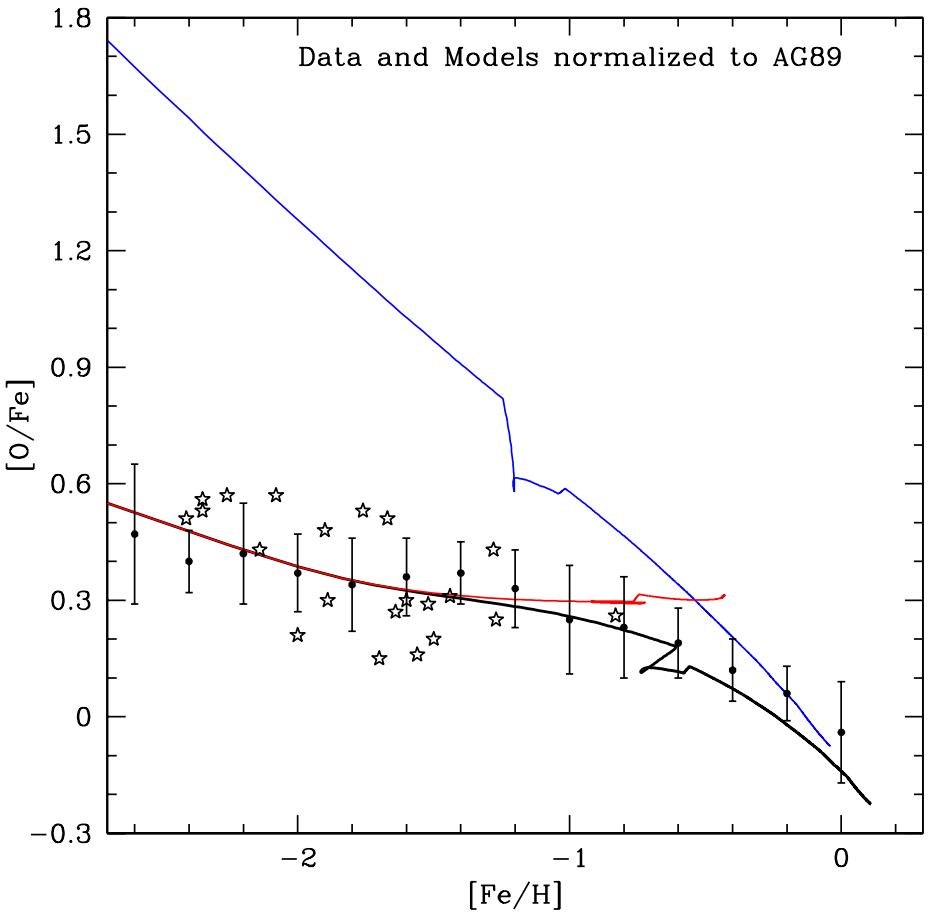

Fig. 1.3. Time-delay model. The models and the data are normalized to the solar meteoritic abundances of Anders & Grevesse (1989). The thick curve represents the predictions of the standard time-delay model where SNe Ia produce 70% of Fe and SNe II produce the remaining 30%. The figure is from Matteucci & Chiappini (2004). The data are all from Meléndez & Barbuy (2002).

1.11 Common Conclusions from Galaxy Models

Most of the more recent chemical evolution models agree on several important issues.

(1) The G-dwarf metallicity distribution can be reproduced only by assuming that the formation of the local disk occurred by infall of extragalactic gas on a long time scale, of the order of $\tau_D \sim 6-8$ Gyr (Chiappini et al. 1997; Boissier & Prantzos 1999; Chang et al. 1999; Alibès, Labay, & Canal 2001; Chiappini et al. 2001). Previous authors had already suggested a time scale of a few (1–3) Gyr for the formation of the Galactic disk (among others, Larson 1969; Lynden-Bell 1975; Yoshii & Saio 1979; Pagel 1989).

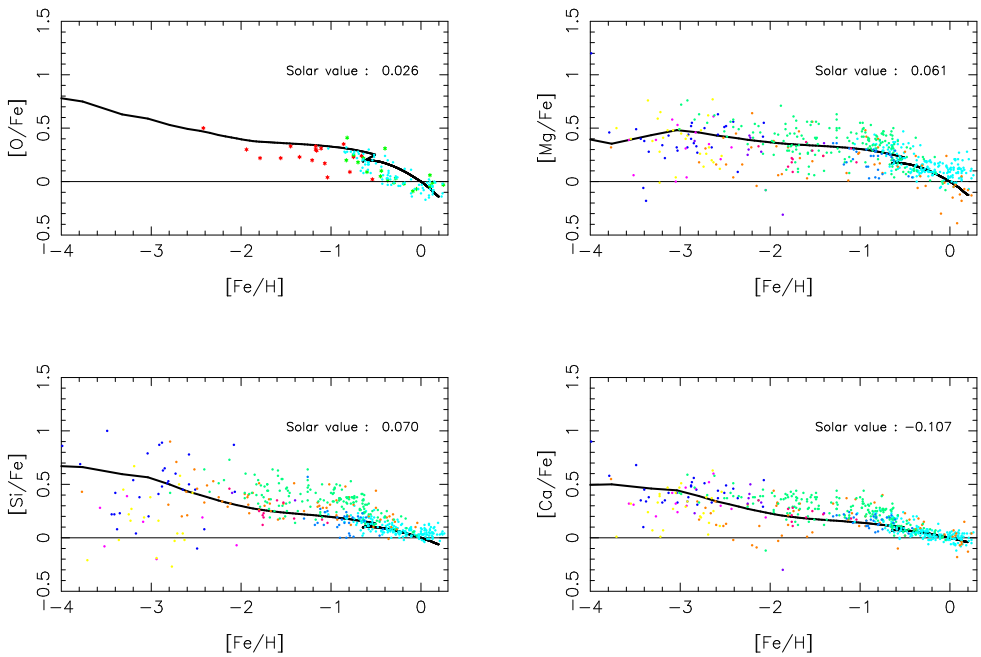

Fig. 1.4. Predicted and observed [α/Fe] vs. [Fe/H] in the solar neighborhood. The models and the data are from François et al. (2004). The models are normalized to the predicted solar abundances. The predicted abundance ratios at the time of the formation of the Sun are shown in each panel and indicate a good fit.

(2) The relative abundance ratios [X_i/Fe] vs. [Fe/H], interpreted as being due to time delay between SNe Ia and SNe II, allow one to reproduce the observed relations (see Fig. 1.4) and to infer the time scale for the halo-thick disk formation (corresponding to [Fe/H] = −1.0), which should be of the order of $\tau_H \approx 1.5$ Gyr (Matteucci & Greggio 1986; Matteucci & François 1989; Chiappini et al. 1997). On the other hand, the external halo formed more slowly, perhaps on time scales of the order of 3–4 Gyr (see Matteucci & François 1992). In Figure 1.4 we show the predictions of the model developed by Chiappini et al. (1997), by adopting the yields of Woosley & Weaver (1995) for SNe II* and those of Nomoto et al. (1997) for SNe Ia (their case W7). The Mg yield in SNe Ia also had to be increased in order to fit the solar abundances (François et al. 2004). The problem of Mg underproduction in nucleosynthesis models is well known, as was pointed out by Thomas, Greggio, & Bender (1998). Figure 1.4 shows clearly that the agreement between the model predictions and data for α-elements is quite good and support the time-delay model.

(3) To fit abundance gradients and SFR and gas distributions along the disk, the disk should have formed inside-out (variable τ_D), and the SFR should be a strongly varying function of the galactocentric distance, as in Equations (1.4)–(1.6) (Matteucci & François 1989; Chiappini et al 1997, 2001; Portinari & Chiosi 1999; Goswami & Prantzos 2000; Alibés et al. 2001).

* With the exception of the Mg yields, which have been artificially increased by a factor of 5 to obtain a good agreement with the solar abundance of Mg.

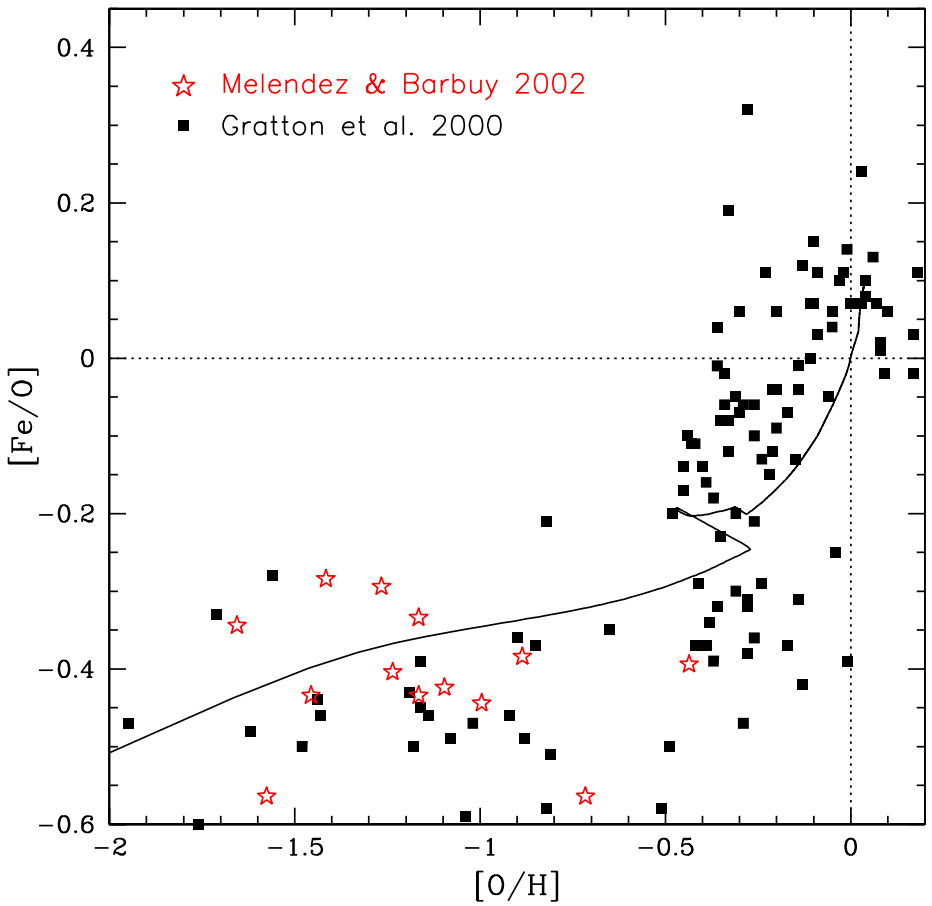

Fig. 1.5. Gap in the SFR. The model predictions for [Fe/O] vs. [Fe/H] are obtained by means of the two-infall model (see text). As one can see, a gap seems to be evident at [O/H] $\approx$ –0.3.

1.12 Specific Conclusions from Galaxy Models

The assumed threshold in the SFR (Chiappini et al. 1997) produces naturally a gap in the star formation process between the end of the halo-thick disk phase and the beginning of the thin disk phase. Such a gap lasts for $\sim$1 Gyr, and it seems to be indicated by the observations (Gratton et al. 2000). In particular, in Figure 1.5 we show the observed and predicted [Fe/O] vs. [O/H], where it appears that at around [O/H]= –0.3 there is a lack of stars and then the [Fe/O] ratio rises sharply. This is a clear indication, on the basis of the time-delay model, that there has been a period when only Fe was produced, in other words a halt in the SFR. This gap seems to be observed also in the [Fe/Mg] vs. [Mg/H] (Furhmann 1998). However, more data are necessary before drawing firm conclusions on this important point (see also Chiappini & Matteucci 2004).

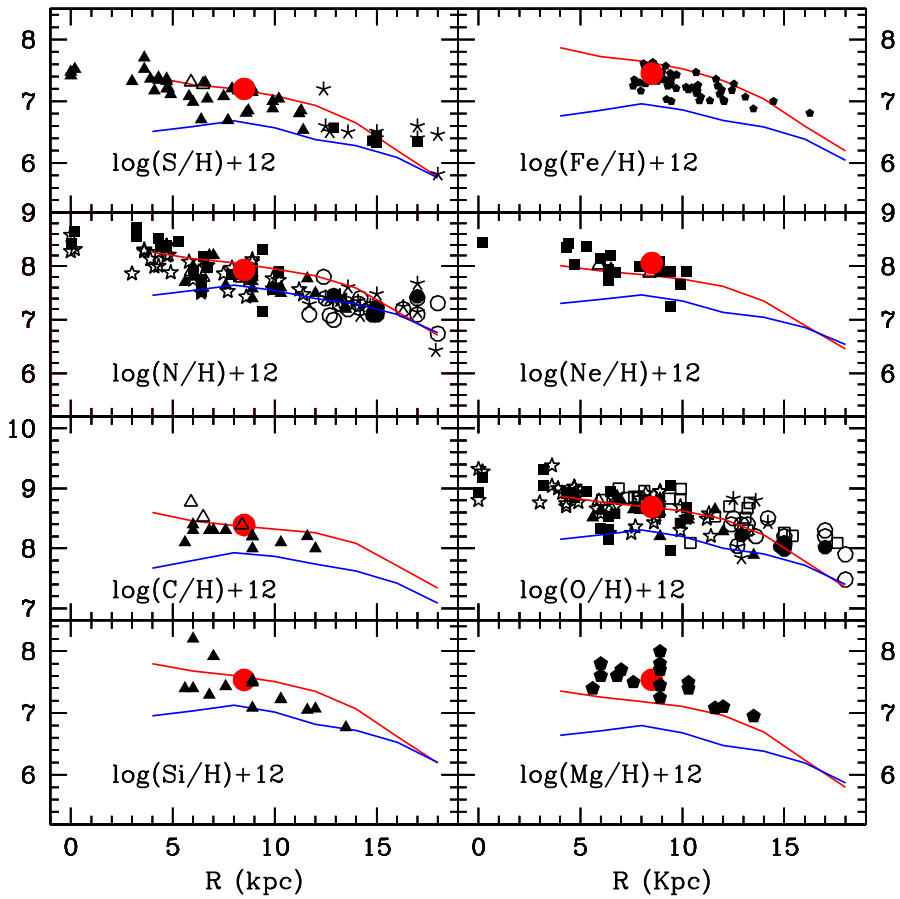

Fig. 1.6. Abundance gradients along the Galactic disk and their evolution in time, as predicted by the model of Chiappini et al. (2001), where all the references to the data can be found. The lower curve of each panel represents the model prediction after 2 Gyr from the beginning of star formation in the thin disk. The upper curve represent the predicted gradient at the present time.

No agreement on the behavior of gradients in time exists among different authors. In particular, some authors (e.g., Boissier & Prantzos 1999; Portinari & Chiosi 1999; Alibès et al. 2001) find a flattening of abundance gradients with time, whereas others (Matteucci & François 1989; Chiappini et al. 2001; see Fig. 1.6) predict a steepening of the abundance gradients, in agreement with results from chemo-dynamical models (Samland, Hensler, & Theis 1997). The difference between the two different approaches assumed by the various authors could perhaps reside in the different star formation and/or infall laws adopted for the Galactic disk (see Tosi 2000 for a discussion of this point). Data from planetary nebulae of different ages can help in solving this problem; recently, Maciel, Costa, & Uchida (2002)

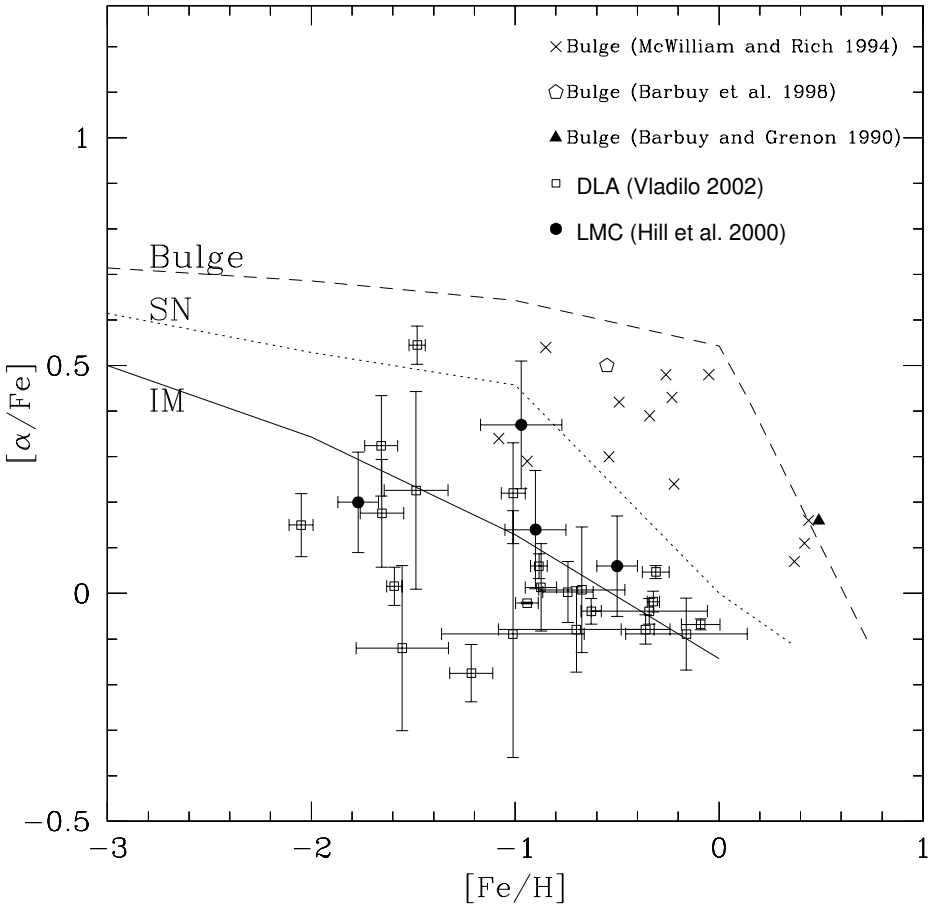

Fig. 1.7. The predicted [α/Fe] vs. [Fe/H] in different objects. Data for the Galactic bulge, the LMC, and damped Lyα systems are shown for comparison.

suggested a flattening of the gradients with time. In any case, all the models predict a very small evolution in the last 5 Gyr.

1.13 Star Formation Rate in Galaxies

It is very important to understand that different histories of star formation determine the abundance patterns in galaxies. In particular, the [X_i/Fe] vs. [Fe/H] relations are strongly influenced by the SFR, which influences the temporal growth of the Fe abundance.

In other words, the time-delay model coupled with different star formation histories implies different time scales for the bulk of Fe production from SNe Ia, thus producing different [α/Fe] vs. [Fe/H] relations in different objects. The typical time scale for SN Ia enrichment can be defined as the time when the SN Ia rate reaches the maximum t_{SNIa} (Matteucci & Recchi 2001). This time scale depends upon the progenitor lifetimes, the IMF, and the SFR.

For an elliptical galaxy or a bulge of a spiral with high SFR, the maximum in the SN Ia rate is reached at $t_{SNIa} = 0.3-0.5$ Gyr, whereas for a spiral like the Milky Way a first maximum in the SN Ia rate is reached at $t_{SNIa} = 1.5$ Gyr and a second maximum, if one uses the two-infall model, at $t_{SNIa} = 4-5$ Gyr. Therefore, for the Milky Way 1–1.5 Gyr is the time at which SNe Ia are no longer negligible in the process of chemical enrichment, and it corresponds to the change in slope observed in the [el/Fe] vs. [Fe/H] relations (Fig. 1.4) and to the end of the halo phase. For an irregular galaxy, where the SFR is assumed to proceed more slowly than in the solar vicinity, the time scale for SN Ia enrichment is $t_{SNIa} = 7-8$ Gyr. Therefore, it is worth repeating that t_{SNIa} is different in different galaxies, since often in the literature it is adopted as a universal time scale of 1 Gyr! On the basis of that, we expect that objects where the SFR proceeds very fast, such as in the spheroids (bulges and ellipticals), the [α/Fe] ratio stays flat for a larger metallicity interval than in systems with slower star formation, such as the Milky Way, and that eventually the [α/Fe] ratios in irregulars, where the star formation rate has been less efficient than in spirals, decreases almost continuously, as shown in Figure 1.7. The models shown in Figure 1.7 contain the same nucleosynthesis prescriptions and differ in the star formation history.

1.14 High-redshift Objects

In Figure 1.7 we show also some observational data relevant to the Galactic bulge, the LMC, and some damped Lyα systems. As one can see, our predictions seem to reproduce the data for the Galactic bulge and for LMC. They also suggest that damped Lyα systems could be the progenitors of the present-day irregular galaxies, since most damped Lyα systems, once their abundances are corrected for the effect of dust, show low [α/Fe] ratios at low metallicities (Vladilo 2002; Calura, Matteucci, & Vladilo 2003). On the other hand, Lyman-break galaxies such as cB58 (Pettini et al. 2002) show an abundance pattern compatible with a young spheroid, either a galactic bulge or a small elliptical, experiencing a galactic outflow, as recently shown by Matteucci & Pipino (2002). Therefore, the [X_i/Fe] vs. [Fe/H] diagram represents a very useful tool to infer the nature of high-redshift objects, for which we know just the abundances and abundance ratios.

References

Alibés, A., Labay, J., & Canal, R. 2001, A&A, 370, 1103
Anders, E., & Grevesse, N. 1989, Geochim. Cosmochim. Acta, 53, 197
Argast, D., Samland, M., Gerhard, O. E., & Thielemann, F.-K. 2000, A&A, 356, 873
Boissier, S., & Prantzos, N. 1999, MNRAS, 307, 857
Calura, F., Matteucci, F., & Vladilo, G. 2003, MNRAS, 340, 59
Chang, R. X., Hou, J. L., Shu, C. G., & Fu, C. Q. 1999, A&A, 350, 38
Chiappini, C., & Matteucci, F. 2004, in Carnegie Observatories Astrophysics Series, Vol. 4: Origin and Evolution of the Elements, ed. A. McWilliam & M. Rausch (Pasadena: Carnegie Observatories, http://www.ociw.edu/symposia/series/symposium4/proceedings.html)
Chiappini, C., Matteucci, F., & Gratton, R. 1997, ApJ, 477, 765
Chiappini, C., Matteucci, F., & Padoan, P. 2000, ApJ, 528, 711
Chiappini, C., Matteucci, F., & Romano, D. 2001, ApJ, 554, 1044
Chiosi, C. 1980, A&A, 83, 206
Dopita, M. A., & Ryder, S. D. 1994, ApJ, 430, 163
Elmhamdi, A., Chugai, N. N., & Danziger, I. J. 2003, A&A, 404, 1077
François, P., Matteucci, F., Cayrel, R., Spite, M., Spite, F., & Chiappini, C. 2004, A&A, submitted
Fuhrmann, K. 1998, A&A, 338, 161
Goswami, A., & Prantzos, N. 2000, A&A, 359, 191

Gratton, R. G., Carretta, E., Matteucci, F., & Sneden, C. 2000, A&A, 358, 671
Greggio, L., & Renzini, A. 1983a, A&A, 118, 217
——. 1983b, Mem. Soc. Ast. It., 54, 311
Kennicutt, R. C., Jr. 1998, ApJ, 498, 541
Kroupa, P., Tout, C. A., & Gilmore, G. 1993, MNRAS, 262, 545
Hachisu, I., Kato, M., & Nomoto, K. 1999, ApJ, 522, 487
Hartwick, F. 1976, ApJ, 209, 418
Hill, V., François, P., Spite, M., Primas, F., & Spite, F. 2000, A&A, 364, L19
Iben, I., Jr., & Tutukov, A. V. 1984, ApJS, 54, 335
Iwamoto, K., Brachwitz, F., Nomoto, K., Kishimoto, N., Umeda, H., Hix, W. R., & Thielemann, F.-K. 1999, ApJS, 125, 439
Landau, L. D., & Lifshitz, E. M. 1962, Quantum Mechanics (London: Pergamon)
Langer, N., & Henkel, C. 1995, Space Sci. Rev., 74, 343
Larson, R. B. 1969, MNRAS, 145, 405
——. 1998, MNRAS, 301, 569
Limongi, M., & Chieffi, A., 2003, ApJ, 592, 404
Lynden-Bell, D. 1975, Vistas in Astronomy, 19, 299
Maciel, W., Costa, R. D. D., & Uchida, M. M. M. 2003, A&A397, 667
Maeder, A. 1992, A&A, 264, 105
Mannucci, F., et al. 2003, A&A, 401, 519
Marigo, P., Bressan, A., & Chiosi, C. 1996. A&A, 313, 545
Matteucci, F. 1986, ApJ, 305, L81
——. 2001, The Chemical Evolution of the Galaxy (Dordrecht: Kluwer)
Matteucci, F., & Chiappini, C. 2004, in preparation
Matteucci, F., & Chiosi, C. 1983, A&A, 123, 121
Matteucci, F., & François, P. 1992, A&A, 262, L1
——. 1989, MNRAS, 239, 885
Matteucci, F., & Greggio, L. 1986, A&A154, 279
Matteucci, F., & Pipino, A. 2002, ApJ, 569, L69
Matteucci, F., & Recchi, S., 2001, ApJ, 558, 351
McWilliam, A., & Rich, R. M. 1994, ApJS, 91, 7
Meléndez, J., & Barbuy, B. 2002, ApJ, 575, 474
Meynet, G., & Maeder, A. 2002, A&A, 390, 561
Nakamura, T., Umeda, H., Iwamoto, K., Nomoto, K., Hashimoto, M., Hix, W. R., & Thielemann, F.-K. 2001, ApJ, 555, 880
Nomoto, K., Iwamoto, K., Nakasato, N., Thielemann, F.-K., Brachwitz, F., Tsujimoto, T., Kubo, Y., & Kishimoto, N. 1997, Nuc. Phys. A, 621, 467
Oey, M. S. 2000, ApJ, 542, L25
Pagel, B. E. J. 1989, in Evolutionary Phenomena in Galaxies, ed. J. E. Beckman & B. E. J. Pagel (Cambridge: Cambridge Univ. Press), 201
Pardi, M. C., Ferrini, F., & Matteucci, F. 1995, ApJ, 444, 207
Pettini, M., Rix, S. A., Steidel, C. C., Adelberger, K. L., Hunt, M. P., & Shapley, A. E. 2002, ApJ, 569, 742
Portinari, L., & Chiosi, C. 1999, A&A, 350, 827
Portinari, L., Chiosi, C., & Bressan, A. 1998, A&A, 334, 505
Prantzos, N. 2003, in The Evolution of Galaxies III: From Simple Approaches to Self-Consistent Models, ed. G. Hensler et al. (Dordrecht: Kluwer), 381
Rauscher, T., Hoffman, R. D., & Woosley, S. E. 2002, ApJ, 576, 323
Salpeter, E. E. 1955, A&A, 121, 161
Samland, M., Hensler, G., & Theis, C. 1997, ApJ476, 544
Scalo, J. M. 1986, Fund. Cosmic Phys., 11, 1
——. 1998 in The Stellar Initial Mass Function, ed. G. Gilmore, I. Parry, & S. Ryan (San Francisco: ASP), 201
Schmidt, M. 1959, ApJ, 129, 243
Siess, L., Livio, M., & Lattanzio, J. 2002, ApJ, 570, 329
Talbot, R. J., & Arnett, D. W. 1971, ApJ, 170, 409
Thielemann, F.-K., Nomoto, K., & Hashimoto, M. 1996, ApJ, 460, 408
Tinsley, B. M. 1979, ApJ, 229, 1046
——. 1980, Fund. Cosmic Phys., 5, 287

Thomas, D., Greggio, L., & Bender, R. 1998, A&A, 296, 119
Tornambé, A., & Matteucci, F. 1986, MNRAS, 223, 69
Tosi, M. 1988 A&A197, 33
——. 2000, in The Chemical Evolution of the Milky Way: Stars versus Clusters, ed. F. Matteucci & F. Giovannelli (Dordrecht: Kluwer), 505
Tsujimoto, T., Shigeyama, T., & Yoshii, Y. 1999, ApJ, 519, L63
Umeda, H., & Nomoto, K. 2002, ApJ, 565, 385
van den Hoek, L. B., & Groenewegen, M. A. T. 1997 A&AS, 123, 305
Ventura, P., D'Antona, F., & Mazzitelli, I. 2002, A&A, 393, 21
Vladilo, G. 2002, A&A, 391, 407
Whelan, J., & Iben, I., Jr. 1973, ApJ, 186, 1007
Woosley, S. E., & Weaver, T. A. 1995, ApJS, 101, 181
Wyse, R. F. G., & Silk, J. 1989, ApJ, 339, 700
Yoshii, Y., & Saio, H. 1979, PASJ, 31, 339